Self-Cleaning Surfaces Realized by Biologically Sized Magnetic Artificial Cilia

Self-Cleaning Surfaces Realized by Biologically Sized Magnetic Artificial Cilia

Zhiwei Cui, Shuaizhong Zhang, Ye Wang, Laura Tormey, Olivia S. Kanies, Richard Chasen Spero, Jay K. Fisher, and Jaap M. J. den Toonder*

Magnetic artificial cilia (MAC) are small actuators inspired by biological cilia found in nature. In microfluidic chips, MAC can generate flow and remove microparticles, with applications in anti-fouling. However, the MAC used for anti-fouling in the current literature has dimensions of several hundred micrometers in length, which limits the application to relatively large length scales. Here, biologically-sized magnetic artificial cilia (b-MAC) which are only 45 micrometers long and that are randomly distributed on the surface, are used to remove microparticles. It is shown that microparticles with sizes ranging from 5 to 40 µm can be removed efficiently and the final cleanness ranges from 69% to 100%, with the highest cleanness for the highest actuation frequency applied (40 Hz). The lowest cleanness is obtained for microparticles with a size equal to the average pitch between the b-MAC. The randomness in cilia distribution appears to have a positive effect on cleanliness, compared with the authors' earlier work using a regular cilia array. The demonstrated self-cleaning by the b-MAC constitutes an essential step toward efficient self-cleaning surfaces for real-life application in miniaturized microfluidic devices, such as lab-on-a-chip or organ-on-a-chip devices, as well as for preventing fouling of submerged surfaces such as marine sensors.

1. Introduction

Fouling, being the accumulation of undesired contaminants such as organic molecules, cells, and microparticles on a submerged surface, forms a problem for many applications.[1,2] One example of

Z. W. Cui, S. Z. Zhang, Y. Wang, J. M. J. den Toonder
Department of Mechanical Engineering
Eindhoven University of Technology
P.O. Box 513, Eindhoven 5600 MB, The Netherlands
E-mail: J.M.J.d.Toonder@tue.nl
Z. W. Cui, S. Z. Zhang, Y. Wang, J. M. J. den Toonder
Institute for Complex Molecular Systems
Eindhoven University of Technology
Eindhoven 5612 AJ, The Netherlands
L. Tormey, O. S. Kanies, R. C. Spero, J. K. Fisher
Redbud Labs Inc.
Research Triangle Park, NC 27709, USA

The ORCID identification number(s) for the author(s) of this article can be found under https://doi.org/10.1002/admi.202102016.

such an application is lab-on-a-chip devices, as the absorption of microparticles, cells of molecules to the device walls, or the accumulation of these contaminants in microfluidic channels, inhibits normal device operation, for example, causing microchannel clogging.[3] Another example are submerged sensor surfaces for environmental monitoring in oceans, lakes, or rivers, or in chemical and food processing operations, where fouling can lead to reduced sensitivity and/or lifetime.[4] To date, chemical and physical mechanisms form the main strategies to tackle (bio)fouling problems, for example, using synthetic chemical coatings or introducing surface topographies to modulate surface energy and wetting.[5,6] Most of these mechanisms are static, and aimed at deterring initial adsorption and attachment of fouling agents; they especially work well in a flow environment. In the case of little external flow, however, gravity or diffusive mechanisms cause sedimentation and accumulation of fouling agents, and the static surfaces lack the option to actively repel the contaminants, so they need to be combined with disruptive and time-consuming cleaning protocols.[3,7] Inspired by nature, researchers have recently developed artificial cilia[7,8] that can be actuated to actively perform surface cleaning by generating flow, which can be effective for anti-fouling especially in conditions with little external flow.[7,9]

Biological cilia are tiny flexible hair-like structures that are ubiquitous in nature. The typical size of small biological cilia is ≈10 µm in length and 200 nm in diameter.[7,10–13] They perform various functions such as fluid actuation, chemical and mechanical sensing, surface energy modification, and feeding.[7,9,14–20] For example, the cilia present in our lungs and lower respiratory tract act to remove dust particles and mucus from our airways.[21–24] Inspired by nature, in recent years, researchers have created and studied artificial cilia for applications such as pumping, mixing, and particle manipulation based on a multitude of numerical studies.[9,14–20,25,26] According to previously published numerical simulation analyses, cilia surfaces have promising advantages for removing deposited microparticles.[27–33] Inspired by these numerical studies, Zhang et al. recently used magnetic artificial cilia to effectively remove microparticles from surfaces experimentally.[7] However, the cilia used in that research were 350 µm in length and 50 µm in diameter, which is much larger than biological cilia. This limits their application to relatively large devices. Furthermore, the cilia array in the publication

mentioned previously is aligned in a regular patten, which can limit the self-cleaning capabilities. In particular, it was found that when the particle sizes are close to the cilia pitch (the spacing of adjacent cilia), the cleaning effectiveness is reduced.[7]

In this work, we use Redbud Posts, a type of magnetic artificial cilia manufactured by Redbud Labs (Research Triangle Park NC, USA) that are one order of magnitude smaller than MAC used in our prior work on self-cleaning surfaces (i.e., 45 µm in length, 3.5 to 4 µm in diameter), close to biological cilia lengths, and we perform microparticle removal experiments. Moreover, our Redbud Posts are randomly distributed rather than placed in a regular array. These biologically sized magnetic artificial cilia – b-MAC – can be actuated by an external magnetic field. The b-MAC arrays were integrated into a microchamber to evaluate the capability of cleaning microparticles with diameters in the range of 5 to 40 µm, which is close to the biological-sized microparticles.[34–36] We demonstrate effective self-cleaning by the biologically sized artificial cilia, and therefore, our results constitute an essential step toward efficient self-cleaning surfaces for real-life application in miniaturized microfluidic devices.

2. Results and Discussion

2.1. B-MAC Actuation and Motion

The b-MAC were actuated by a homebuilt rotating magnetic setup as shown in **Figure 1**a. Detailed information about the setup can be found in the Experimental Section. The b-MAC have a length of 45 µm and a diameter of 3.5 to 4 µm. They are distributed randomly over the surface, at an average pitch of 30 µm (calculated according to the b-MAC areal density provided, 100 000 cm^{-2}). A patch of b-MAC (≈3 mm × 3 mm) is integrated into a circular microchannel with a width and height of 5 mm and 390 µm, respectively, as sketched in Figure 1b. Note that the Figure is a schematic one, which means that it is not to scale.

Actuated by the rotating magnet, the b-MAC performs a tilted conical motion as shown schematically in Figure 1c. This motion consists of two parts: an effective stroke, where the cilia pass through an upright position, and a recovery stroke, where they are tilted close to the substrate. Due to the difference in hydrodynamic drag between the two strokes, a net flow can be created in the direction of the effective stroke. In our experiments, the relative orientation of the microfluidic channel and the magnet is such that the effective stroke is in the direction tangential to the channel. Figure 1d is a stacked top-view image of the b-MAC motion over one period when they are actuated at 1 Hz, which confirms that the b-MAC exhibits rotational conical motion. The opening angle of the cone traced by the b-MAC is ≈75° at 1 Hz, whereas the tilting angle of the cone axis with respect to the surface is ≈53°. The opening angle of the b-MAC for different frequencies is shown in Figure 1e. According to the plot, the opening angle remains constant up to 20 Hz, after which it decreases. This is due to the increased viscous drag at higher frequencies which reduces the amplitude of motion as found in previous studies as well.[22,37] Movie S1, Supporting Information, is a video recording of the b-MAC motion at 1 Hz.
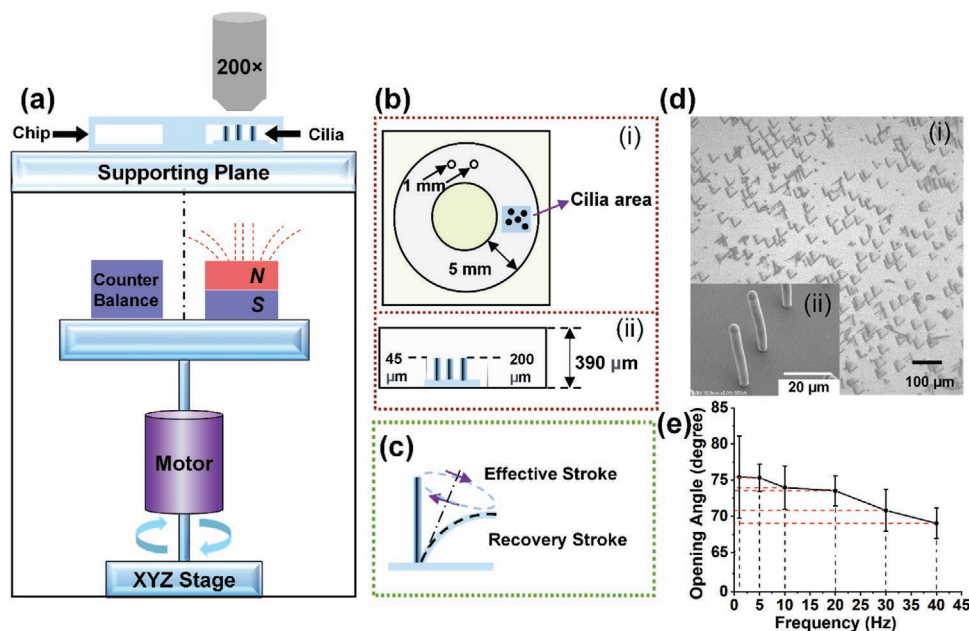
Figure 1. Experimental setup and the motion of the biological-sized magnetic artificial cilia, b-MAC. a) Homebuilt rotating magnet-setup. The position of the electric motor and permanent magnet can be regulated by the XYZ stage at the bottom. The center of the permanent magnet has an offset relative to the rotational axis of the motor. b) Schematics of the i) top and ii) side view of the microfluidic chip with an integrated b-MAC patch, as used in the experiments (not to scale). c) Schematic of the b-MAC motion under actuation by the rotating magnetic setup. A complete period can be seen to have two strokes: an effective stroke when the b-MAC is almost perpendicular to the substrate, and a recovery stoke when it is moving back in a trajectory closer to the surface. d-i) Superposition of top view images taken in one period of b-MAC motion under an actuation frequency of 1 Hz (see Movie S1, Supporting Information). ii) Scanning electron microscopy (SEM) image of the b-MAC fabricated. For taking the SEM image, the stage was tilted 30°. The b-MAC themselves have a slight tilt of ≈5° due to the preparation for SEM. e) Opening angle of b-MAC at different actuation frequencies. All error bars are standard deviations of the obtained data of at least three measurements.

ADVANCED
SCIENCE NEWS
www.advancedsciencenews.com

ADVANCED
MATERIALS
INTERFACES
www.advmatinterfaces.de

2.2. Effect of Particle Size on Cleaning

Polystyrene (PS) particles with diameters ranging from 5 to 40 µm were used to evaluate the effect of microparticle size on the cleanness at an actuation frequency of 40 Hz. The reason we chose polystyrene microparticles is that the density of the PS is ≈1.05 g cm^{-3}, which is slightly larger than that of water (1.0 g cm^{-3}). Hence, the particles will not sediment too quickly, because this could influence the measurement accuracy of the cleanness due to the sensitivity to initial conditions of the experiments, the filling procedure, and the quality of the particle dispersion. The particles are still slightly denser than water, to allow for slow sedimentation and accumulation to show the cleaning effect. To compare and evaluate the cleanness from the experimental observations, we define the cleanness at time t as

$$C_t = (N_0 - N_t)/N_0 \tag{1}$$

where C_t is the cleanness of the observation area after an actuation time of t s, N_0 is the initial number of microparticles in the field of view before actuation, and N_t is the number of microparticles remaining at time t. The results are shown in **Figure 2**a. Figure 2b is a graph of cleanness versus average size ratio, defined as the diameter of the microparticles divided by the average pitch between the b-MAC (30 µm). To illustrate the cleaning process, Figure 2c,d are representative images at the

start of the experiment, and after 90 and 300 s of actuation, for 40 and 5 µm microparticles, respectively.

Figure 2 shows, that for all sizes of microparticles (ranging from 5 to 40 µm), the cleanness increases after starting the actuation and reaches a steady state after 60 to 200 s. The highest steady state cleanness (98.6% ± 0.5%) is reached for the microparticles with a diameter of 5 µm, and is obtained within 60 s. The general trend observed is that the steady state cleanness reduces for larger particle sizes. The lowest steady state cleanness (69% ± 0.5%) is however reached for the 30 µm microparticles, for which the diameter equals the average pitch of the b-MAC array.

The steady state cleanness is in general lower than 100%, that is, no fully cleaned surface is obtained. The reasons are as follows. (1) All groups of microparticles contain a portion for which the microparticle diameter is similar to some of the actual pitches of the b-MAC, and therefore, some of the microparticles remain stuck between the b-MAC at the steady state. This phenomenon occurs in all the experiments because the b-MAC are randomly distributed. (2) Because of the random b-MAC distribution, the flow field generated by the b-MAC is irregular, including many local vortices (see Movies S2 and S3, Supporting Information). Consequently, some of the microparticles are trapped in these local vortices at the final steady state and cannot escape, even for a prolonged actuation time. The corresponding video of the final state of the 40 µm-sized microparticles, illustrating this phenomenon, is available in Movie S3,
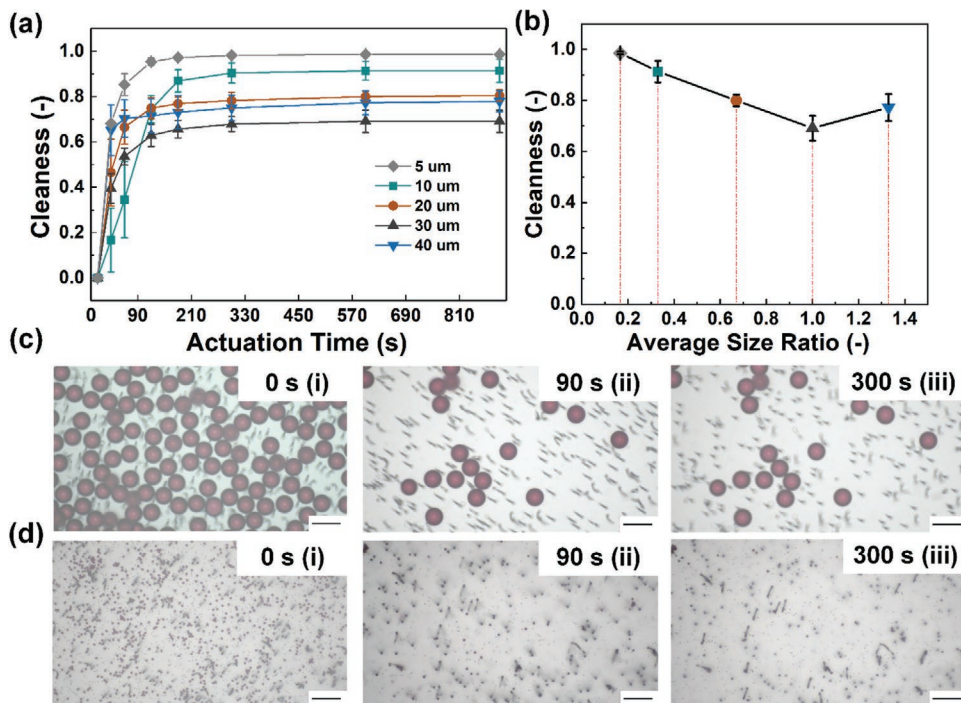
Figure 2. Cleaning of microparticles of different sizes using b-MAC. a) Cleanness values as a function of actuation time at a frequency of 40 Hz for different microparticle sizes. b) The final cleanness after an actuation time of 300 s, versus the average size ratio, which is defined as the ratio of the microparticle diameter and average cilia pitch. c,d) Snapshots during the cleaning process of microparticles with a diameter of c) 40 µm and d) 5 µm at the i) start of the experiment, ii) after 90 s, and iii) 300 s of actuation, respectively. The corresponding videos showing microparticle removal can be found in Movies S2 and S3, Supporting Information. The scale bars in (c,d) are 50 µm long. The error bars represent one standard deviation from three independent experiments. Note: All cleaning experiments reported in this figure lasted 900 s (15 min). During this time, no loss of the b-MAC function was observed. From previous research, we know that the Redbud posts that form our b-MAC can be actuated at 6000 rpm for days without any loss of function or visible damage.[39]

Supporting Information. Note: Since the observed microparticle behavior in the final steady states is similar for all the microparticle sizes, here we only show 40 µm-sized microparticles as an example.

The observation that the 5 µm-sized microparticles can easily be removed and reach the highest cleanness compared to the larger microparticles, can be explained by considering the various forces acting on the microparticles. Three main forces act on the microparticles during the cleaning process. One is the hydrodynamic force induced by the fluid flow generated by actuated b-MAC. Another is the adhesion force acting between the microparticles and the silicone surfaces. Finally, the microparticles experience a mechanical force caused by the direct interaction with the actuated b-MAC. As the actuation frequency is the same for all experiments shown in Figure 2 (i.e., 40 Hz), similar flow profiles are generated by the b-MAC, hence the effect of hydrodynamic forces is expected to be similar for all microparticle sizes. The adhesion force acting on the microparticles can be described by:[38]

$$F_{adhesion} = 4\pi R \sqrt{\gamma_1 \gamma_2} \tag{2}$$

where R is the radius of the microparticles, and γ_1 and γ_2 are the surface energy of the microparticles and the silicone surface, respectively. Therefore, the adhesion force is proportional to the radius of the microparticles R. Hence, the adhesion forces acting on 5 µm-sized microparticles are smaller than those on the larger ones. As the actuation frequency is the same for all particle sizes in Figure 2, the mechanical force from direct interaction with the b-MAC is the same as well. Moreover, the 5 µm-sized microparticles are more likely to interact directly with the b-MAC because the number of the microparticles is higher than for the larger microparticles. Taken together, the force resulting from the sum of the mechanical force and the hydrodynamic force more likely overcomes the adhesion force for smaller than for larger microparticles. In addition, because the 5 µm microparticles are much smaller than the cilia pitch, they are much less likely to get stuck between cilia. Even if two or more of the 5 µm microparticles form small clusters, they can still be removed (see Movie S2, Supporting Information).

When the microparticles have the same diameter as the average cilia pitch, that is, 30 µm, we obtain the lowest value for the cleanness, as can be seen in Figure. 2b. This is because of more microparticles getting trapped between the b-MAC than for the other sizes. The presence of the trapped microparticles can then restrict the b-MAC motion (see Movie S4, Supporting Information), leading to a decrease of flow generation. Consequently, the hydrodynamic force is weakened, which will make it difficult to overcome the adhesion force. This finding is in agreement with Zhang et al. who used magnetic artificial cilia arranged in a regular array.[7] Note that the cilia in that work were about one order of magnitude larger than our b-MAC, which could in principle, influence the cleaning results. Nonetheless, it is still meaningful to compare our results with those of Zhang et al. when we use the ratio between the particle size and the cilia pitch (either regular or average) as a non-dimensional parameter. As shown in Figure. 2b, the lowest value of cleanness we reach here (69% ± 0.5%) is substantially higher than that found by Zhang et al. (≈40%). This is likely caused

by the fact that in a regular array, the particles may get trapped between the cilia anywhere on the cilia surface if their size equals the cilia pitch, while in an irregular array, the cilia pitch will be equal to the particles size only in a small portion of the entire cilia area so that the particles will get trapped between cilia only in certain locations. These results indeed suggest that the random distribution of the b-MAC array helps to improve the overall cleanness.
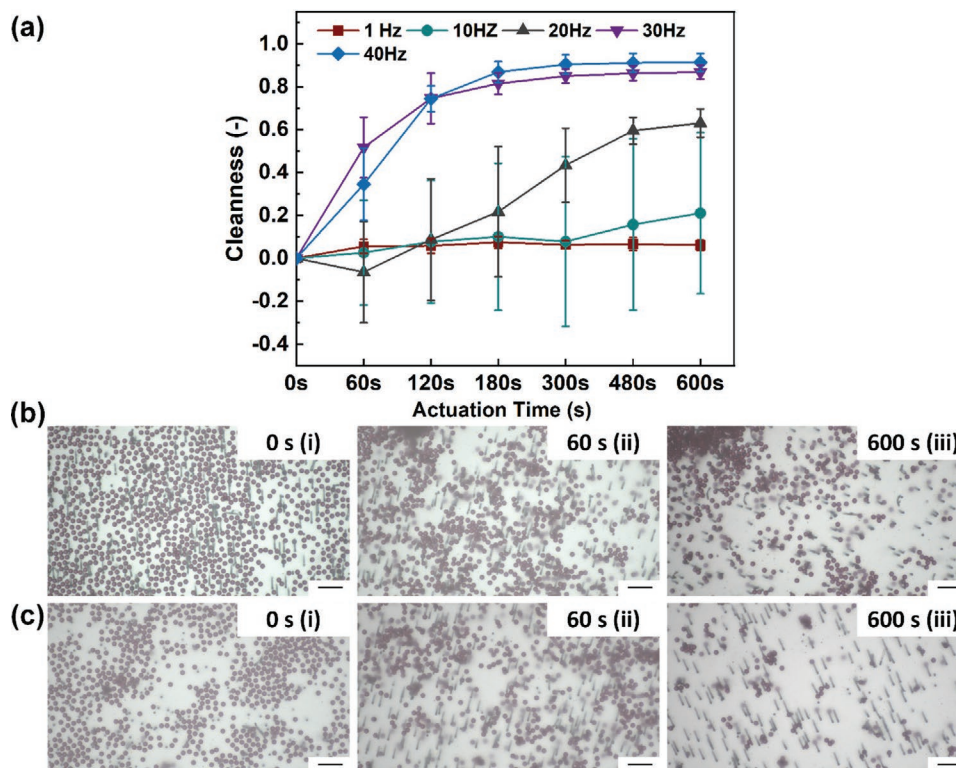
2.3. Effect of Actuation Frequency on Cleaning

To evaluate the effect of actuation frequency on the cleaning ability of the b-MAC, we used 10 µm-sized microparticles. The resulting time-evolution of the cleanness at different actuation frequencies is shown in **Figure** 3a. Figure 3b,c are snapshots during the cleaning at actuation frequencies of 10 and 20 Hz, at the start of the experiment, and after 60 and 600 s, respectively.

The general trend from Figure 3 is that higher actuation frequencies result in better cleaning, with the cleanness at 40 Hz reaching to almost 100%. Explanations for this phenomenon are as follows. (a) For higher rotation speeds of the b-MAC, the induced fluid flow velocity is increased. This results in higher hydrodynamic forces acting on the microparticles, making it easier to break the adhesion forces between the microparticles and the surface. (b) As mentioned earlier, part of the microparticles is trapped in the vortices between the b-MAC, but for higher flow speeds, the microparticles are more likely to escape from the vortices and flow away from the cilia area.[40]

The two lowest frequencies, 1 and 10 Hz, do not result in any significant cleaning. Moreover, the 10 Hz data have large error bars. The low cleaning is because of the microparticles tending to accumulate at certain locations, as is illustrated in Figure 3b; Movie S5, Supporting Information. The accumulation happens in local vortices trapping the microparticles, while the flow velocity is too low to help the microparticles escape. In addition, the trapped microparticles gradually form clusters during the process, which are more difficult to be removed because of the increasing adhesion force with the surface. Moreover, the large error bar in the 10 Hz data is because of the "negative cleanness" in some parts of the observed area. This means that the number of microparticles in these areas increases rather than decreases, caused by strong accumulations. As this accumulation and corresponding local negative cleanness is local, there are also spots with less accumulation reaching a positive cleanness. This variation results in the large error bar.

For the intermediate frequency, 20 Hz, the cleanness initially shows a decreasing trend, that is, it becomes negative. This trend is caused by microparticles entering the observation area from neighboring areas at a higher rate than microparticles are removed initially from the observation area. Note, that the negative cleanness here is caused by the "passer-by" microparticles rather than by the local accumulation observed for 10 Hz. Figure 3c-ii shows these passer-by microparticles at 60 s. In the corresponding Movie S6, Supporting Information, the phenomenon is also apparent. The passerby microparticles are also present in the 30 and 40 Hz experiments, but in this case the initial rate of removal of microparticles is higher than the

**ADVANCED
SCIENCE NEWS**

www.advancedsciencenews.com

**ADVANCED
MATERIALS
INTERFACES**

www.advmatinterfaces.de

Figure 3. The effect of actuation frequency on microparticle removal. a) The cleanness at different actuation frequencies as a function of the actuation time for 10 µm-sized microparticles. The error bars represent the standard deviation of at least three independent experiments. b) Cleaning process at 10 Hz actuation frequency and c) at 20 Hz actuation frequency for the same microparticles. i,ii,iii) are images taken at the start of the experiment, and after 60 and 600 s of actuation time, respectively. Movies S5 and S6, Supporting Information are videos corresponding to (b,c). The scale bars measure 50 µm.

rate of entry of the passer-by microparticles from the start of the experiment (see Movie S7, Supporting Information).

It is possible to regulate the level of cleanness by tuning actuation frequency. Here we show an example, where the b-MAC were first actuated at 10 Hz for 5 min followed by actuation at 40 Hz for another 5 min. The overall cleanness of the whole observation area over time is shown in **Figure 4**a. As expected, the cleanness increases fast after increasing the rotating speed. To quantify this effect in more detail, we calculated the local cleanness at the region in which the microparticles did accumulate, as shown in Figure 4b. At first, the cleanness is negative because of the accumulation of the microparticles at the actuation frequency of 10 Hz, then once the actuation frequency changes to 40 Hz, the cleanness increases rapidly. Figure 4c shows a specific location in the observation area, at which the microparticles did accumulate at 10 Hz.

This effect, clearly, is due to the increased fluid flow velocity at the higher frequency which allows the microparticles to escape from the vortical accumulation areas. Movie S8, Supporting Information, shows the whole process in time.

2.4. Effect of Changing Actuation Direction on Cleaning

We also found that changing actuation direction can effectively disperse and remove the microparticles accumulated in

local vortices. This can be useful in some situations where it is not possible or desirable to increase the actuation frequency for cleaning, for example, when biological samples are present, which can be sensitive to high shear rates. In this case, the cleanness can also be improved at low actuation frequency by changing the rotation direction of the b-MAC during the cleaning process, rather than increasing the actuation frequency. As shown in **Figure 5**, microparticles can accumulate at certain locations when the b-MAC are only actuated in one direction (in this case, anti-clockwise direction) at 10 Hz in the first 5 min, resulting in an initial worsening in overall cleanness. However, when the actuation direction is reversed (by changing the rotation direction of the magnet), the accumulated microparticles can be dispersed and removed, resulting in improvement both in global and local cleanness. A plausible explanation for this effect is that the vortices are at different locations with different actuation directions, so the microparticles that accumulate when the b-MAC are actuated in one direction will be moved out of the vortex and be carried away by the net flow when the actuation direction is changed. They can, by this hypothesis, be trapped again in another vortex, but most will escape, as shown by the total improvement of cleanness in the experiments. It can be expected that after a few times of switching the actuation direction, a maximum level of cleanness will be reached for that frequency. Movie S9, Supporting Information, is a video of the process.
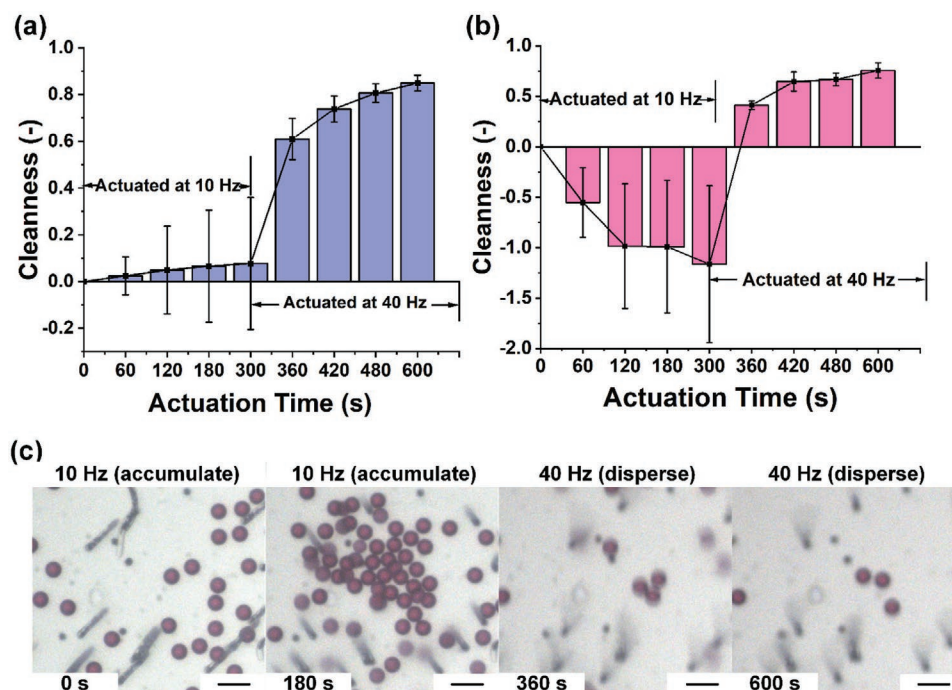
Figure 4. The effect of changing actuation frequency on microparticles' removal. a) Overall cleanness (for the entire observation area) for 10 µm microparticles due to initial b-MAC actuation at 10 Hz, followed by an increase to 40 Hz. b) Local cleanness for a region in which the 10 µm microparticles did accumulate during the initial period of actuation at 10 Hz, followed by an increase in actuation frequency to 40 Hz. c) Video snapshots of the microparticles' removal process in a region where microparticles do accumulate during the first period of actuation at 10 Hz, and during the subsequent actuation period at 40 Hz actuation in which the microparticles are largely removed. The corresponding video is available in Movie S8, Supporting Information. The error bars represent the standard deviation of at least three independent experiments. The scale bars shown in (c) are 20 µm long.

3. Conclusion

In this study, we used magnetic artificial cilia with a size similar to their biological counterparts, b-MAC, with a length of 45 µm, which is suitable for applications at small length scales. The b-MAC were randomly distributed over a surface with an average pitch of 30 µm. We carried out experiments to demonstrate the cleaning capability of b-MAC integrated in a closed microchannel. Microparticles with sizes ranging from 5 to 40 µm could be removed successfully by actuated b-MAC, with a final cleanness from 69% to almost 100% for an actuation frequency of 40 Hz. The resulting cleanness was found to be the worst at 69% when the ratio between the microparticle diameter and the average b-MAC pitch (30 µm in the current experiments) was equal to 1, which was caused by the microparticles getting trapped between b-MAC. Nevertheless, the level of cleanness achieved in this situation was higher than in a previous study, where larger magnetic artificial cilia arranged in regular arrays, and larger microparticles were used. Besides, the cleanness obtained for different actuation frequencies was determined, and as expected, the cleaning was faster for higher frequencies because of the increase of hydrodynamic force. Negative cleanness occurring initially at 20 Hz actuation happened because of "passer-by" microparticles from upstream settling in the observed area. The same effect also happened at higher actuation frequencies, however, the microparticles were quickly cleared away in those situations. Moreover, accumulation of microparticles was observed at low actuation

frequencies, due to microparticle entrapment in local vortices generated by the actuated b-MAC. Besides increasing actuation frequency, we found that reversing the rotation direction of b-MAC, even at the same frequency, turned out to be effective in removing the accumulated microparticles.

In conclusion, it is feasible to realize small-sized microparticle cleaning of surfaces by actuated biologically sized magnetic artificial cilia. This can be useful for applications in lab-on-a-chip and organ-on-a-chip devices, and for preventing fouling of submerged surfaces such as marine sensors and water quality analysers.

4. Experimental Section

b-MAC and Microfluidic Chip Fabrication: Redbud Posts and the associated microfluidic chambers were manufactured by Redbud Labs (Research Triangle Park NC, USA) using a method similar to prior reports.[10,13] Briefly, magnetic material was deposited into a sacrificial template, then backfilled with a hydrophilic silicone elastomer, forming a backing layer ≈125 µm thick. The template had holes with nominal dimensions of 45 µm in depth and 3.75 µm in diameter, allowing the formation of cilia with the same dimensions. After curing, the silicone film was released from the template, exposing the magnetoelastic Redbud Posts. Redbud Post films were then assembled into the microfluidic chips used in the experiment as shown in Figure 1b. The chambers had a closed circular channel with a width of 5 mm, a height of 390 µm, and an overall radius (measured from the geometrical center to the inner channel wall) of 1.5 mm. The b-MAC array was a patch ≈4 × 4 mm within
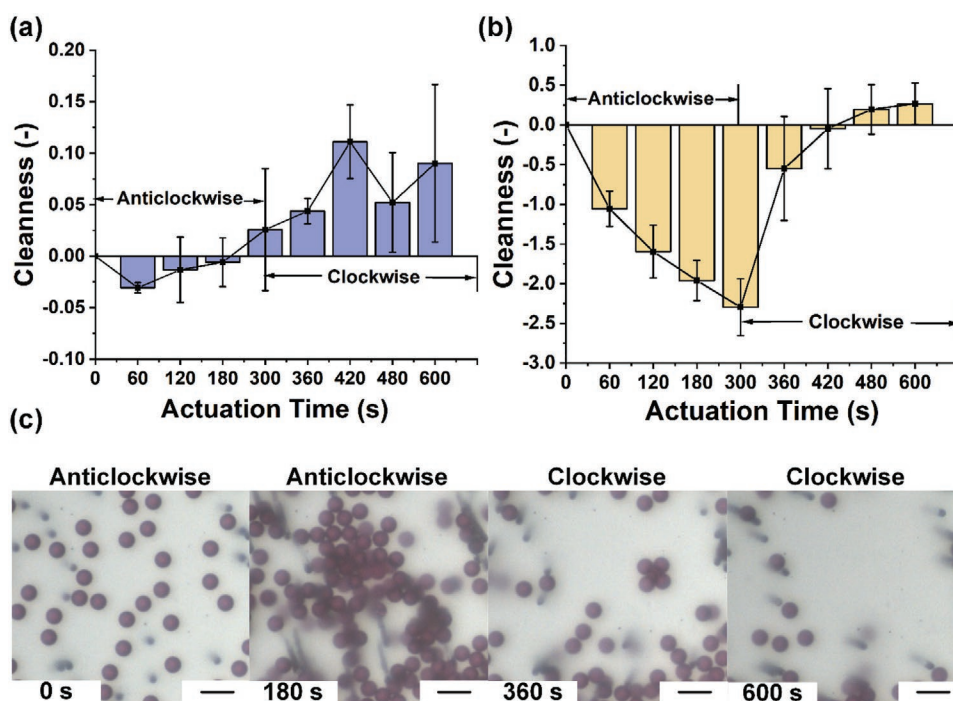
Figure 5. The effect of changing actuation direction on microparticle removal. a) Overall cleanness (for the entire observation area of 640 µm × 360 µm) for 10 µm microparticles for initially anticlockwise b-MAC actuation, followed by a reversal of rotation direction to clockwise (both at 10 Hz). b) Local cleanness measured in specific regions where accumulation of 10 µm microparticles occurred, cropped from the overall image of (a). c) Video snapshots of the microparticle removal process in a region of microparticle accumulation during the first period of actuation in anticlockwise direction, and during the subsequent actuation period in clockwise direction actuation in which the microparticles were largely removed. The corresponding video can be found in Movie S9, Supporting Information. The error bars represent the standard deviation of at least three independent experiments. The scale bars shown in (c) are 20 µm long.

the microchannel. Prior to release, a patch of Redbud Posts (flat silicone side) was mounted to a 1 mm-thick PMMA substrate using pressure sensitive adhesive (PSA). Redbud Posts were then released from the chamber. Separately, the microfluidic chamber with the circular channel was made by laminating 390 µm-thick PSA sidewalls to a PMMA substrate containing a 1 mm inlet and outlet for fluid exchange. Finally, the chamber was mounted on top of the Redbud Post patch, enclosing the MAC in the chamber. The distance from the adhesive backing the Redbud Posts to the tip of the MAC was ≈200 µm, so the vertical space above the b-MAC array was ≈190 µm.

External Actuation Setup: The homebuilt rotating magnetic setup is shown in Figure 1a. It consisted of an XYZ stage, a stepper motor with an encoder, a permanent magnet with a size of 20 × 20 × 10 mm, and a remnant flux density of 1.3 T, a balance weight, and a transparent supporting plane. The relative position of the magnet with respect to the rotation axis and the sample surface could be adjusted. The direction and speed of the motor could be controlled, with a maximum speed of 2400 rpm. The microfluidic chip with integrated b-MAC array was placed on the transparent glass supporting plane (thickness = 1.5 mm). The distance between the surface of the magnet and the bottom surface of the supporting plane was 2 mm. To realize the tilted conical motion of cilia as described above, they were placed at the same offset as the magnet to the rotation axis of the motor. The offset distance between the rotation axis of the motor and the center of the magnet was 6.5 mm.

Microparticles: The microparticles used in this experiment were red polystyrene (PS) microparticles (microparticles GmbH, Germany, 5% w/v in aqueous suspension, density 1.05 g cm^{-3}) with diameters of 5, 10, 20, 30, and 40 µm, respectively. The surface properties of the microparticles were hydrophilic and slightly negatively charged (the zeta potential was in the range of −10 to −12 mV, as provided by the supplier). The 5 and 10 µm-sized microparticles were diluted ten times with deionized water before running the experiment, and the 20,

30, and 40 µm microparticles were used at the original concentration. The surface properties of the cilia and the inner walls of the microfluidic chamber may have had different adhesion properties to the particles. However, in the authors' experiments, no significant difference was observed in particle adhesion between different parts of the chamber.

B-MAC Motion and Cleaning Process: The microparticle solution was injected into the microchannel through the inlet by a 2 mL syringe with a needle of 1 mm. Air bubbles were to be avoided during the proceedings to make sure the whole microchamber was completely full of microparticles solution. After full filling, the inlet and outlet were sealed by a silicone adhesive patch. Initially, a layer of microparticles deposited on the b-MAC area could be observed through a microscope lens (LM Plan FL N 20 ×/0.40, Olympus, Japan), placed above the b-MAC array as indicated in Figure 1a. According to calibration and calculation results, the observation area was 640 µm × 360 µm. B-MAC motions at frequencies, ranging from 1 to 40 Hz, were captured by a high-speed camera (Phantom VEO, USA) with 1000 fps at the actuation frequency of 40 Hz, which was the maximum rotating speed of current magnetic setup. At low actuation frequency, 1 Hz, the capture frame rate was 50 fps. The video can be found in Movie S1, Supporting Information. For the microparticle removal experiments, a CMOS camera (The Imaging Source, DFK 33UX252, Germany) was used with a frame rate of 1 fps. To measure the cleaning effect of the cilia, the numbers of microparticles at specific time points were manually counted after actuating for a time *t*, with varying *t*. Each data point shown in this article was obtained by averaging the results of three repeated experiments.

Supporting Information

Supporting Information is available from the Wiley Online Library or from the author.

Conflict of Interest

The authors declare no conflict of interest.

Data Availability Statement

The data that support the findings of this study are available from the corresponding author upon reasonable request.

[1] M. Přibyl, D. Šnita, M. Marek, *Chem. Eng. J.* **2005**, *105*, 99.
[2] T. Velten, H. Schuck, T. Knoll, O. Scholz, A. Schumacher, T. Göttsche, A. Wolff, B. Z. Beiski, *Proc. Inst. Mech. Eng., Part C* **2006**, *220*, 1609.
[3] R. Mukhopadhyay, *Anal. Chem.* **2005**, *77*, 429 A.
[4] L. Delauney, C. Compare, M. Lehaitre, *Ocean Sci.* **2010**, *6*, 503.
[5] C. M. Kirschner, A. B. Brennan, *Annu. Rev. Mater. Res.* **2012**, *42*, 211.
[6] J. Visser, *Part. Sci. Technol.* **1995**, *13*, 169.
[7] S. Zhang, Y. Wang, P. R. Onck, J. M. J. den Toonder, *Adv. Funct. Mater.* **2019**, *29*, 1900462.
[8] R. M. Judith, J. K. Fisher, R. C. Spero, B. L. Fiser, A. Turner, B. Oberhardt, R. M. Taylor, M. R. Falvo, R. Superfine, *Lab Chip* **2015**, *15*, 1385.
[9] S. Zhang, S. Zhang, P. Zuo, Y. Wang, Y. Wang, P. Onck, J. M. J. D. Toonder, J. M. J. D. Toonder, *ACS Appl. Mater. Interfaces* **2020**, *12*, 27726.
[10] B. A. Evans, A. R. Shields, R. L. Carroll, S. Washburn, M. R. Falvo, R. Superfine, *Nano Lett.* **2007**, *7*, 1428.
[11] T. Xu, J. Zhang, M. Salehizadeh, O. Onaizah, E. Diller, *Sci. Rob.* **2019**, *4*, 29.
[12] J. A. Callow, M. E. Callow, *Nat. Commun.* **2011**, *2*, 244.
[13] A. R. Shields, B. L. Fiser, B. A. Evans, M. R. Falvo, S. Washburn, R. Superfine, *Proc. Natl. Acad. Sci. USA* **2010**, *107*, 15670.
[14] Y. Wang, J. Den Toonder, R. Cardinaels, P. Anderson, *Lab Chip* **2016**, *16*, 2277.
[15] Y. Wang, Y. Gao, H. M. Wyss, P. D. Anderson, J. M. J. den Toonder, *Microfluid. Nanofluid.* **2015**, *18*, 167.
[16] Y. Wang, Y. Gao, H. Wyss, P. Anderson, J. Den Toonder, *Lab Chip* **2013**, *13*, 3360.
[17] S. Zhang, Z. Cui, Y. Wang, J. den Toonder, *Lab Chip* **2020**, *20*, 3569.
[18] S. Zhang, Y. Wang, R. Lavrijsen, P. R. Onck, J. M. J. den Toonder, *Sens. Actuators, B* **2018**, *263*, 614.
[19] S. Zhang, Y. Wang, P. Onck, J. den Toonder, *Microfluid. Nanofluid.* **2020**, *24*, 1.
[20] S. Zhang, R. Zhang, Y. Wang, P. R. Onck, J. M. J. Den Toonder, *ACS Nano* **2020**, *14*, 10313.
[21] S. M. Vanaki, D. Holmes, S. C. Saha, J. Chen, R. J. Brown, P. G. Jayathilake, *J. Biomech.* **2020**, *99*, 109578.
[22] G. R. Fulford, J. R. Blake, *J. Theor. Biol.* **1986**, *121*, 381.
[23] X. M. Bustamante-Marin, L. E. Ostrowski, *Cold Spring Harbor Perspect. Biol.* **2017**, *9*, a028241.
[24] G. J. Pazour, L. Quarmby, A. O. Smith, P. B. Desai, M. Schmidts, *Cell. Signalling* **2019**, *69*, 109519.
[25] E. Milana, R. Zhang, M. R. Vetrano, S. Peerlinck, M. de Volder, P. R. Onck, D. Reynaerts, B. Gorissen, *Sci. Adv.* **2020**, *6*, eabd2508.
[26] S. N. Khaderi, C. B. Craus, J. Hussong, N. Schorr, J. Belardi, J. Westerweel, O. Prucker, J. Rühe, J. M. J. Den Toonder, P. R. Onck, *Lab Chip* **2011**, *11*, 2002.
[27] A. Tripathi, H. Shum, A. C. Balazs, *Soft Matter* **2014**, *10*, 1416.
[28] J. Branscomb, A. Alexeev, *Soft Matter* **2010**, *6*, 4066.
[29] H. Masoud, A. Alexeev, *Soft Matter* **2011**, *7*, 8702.
[30] R. Ghosh, G. A. Buxton, O. B. Usta, A. C. Balazs, A. Alexeev, *Langmuir* **2010**, *26*, 2963.
[31] P. Dayal, O. Kuksenok, A. Bhattacharya, A. C. Balazs, *J. Mater. Chem.* **2012**, *22*, 241.
[32] A. Tripathi, A. Bhattacharya, A. C. Balazs, *Langmuir* **2013**, *29*, 4616.
[33] A. Bhattacharya, G. A. Buxton, O. B. Usta, A. C. Balazs, *Langmuir* **2012**, *28*, 3217.
[34] J. Heyder, J. Gebhart, G. Rudolf, C. F. Schiller, W. Stahlhofen, *J. Aerosol Sci.* **1986**, *17*, 811.
[35] A. Farghadan, K. Poorbahrami, S. Jalal, J. M. Oakes, F. Coletti, A. Arzani, *Comput. Biol. Med.* **2020**, *120*, 103703.
[36] K. Ahookhosh, O. Pourmehran, H. Aminfar, M. Mohammadpourfard, M. M. Sarafraz, H. Hamishehkar, *Eur. J. Pharm. Sci.* **2020**, *145*, 105233.
[37] R. M. Judith, B. Lanham, M. R. Falvo, R. Superfine, *PLoS One* **2018**, *13*, 7.
[38] C. M. Mate, R. W. Carpick, *Tribol. Small Scale*, Oxford University Press, USA **2008**.
[39] J. T. Fisher, T. O. Gurney, B. M. Mason, J. K. Fisher, W. J. Kelly, *Biotechnol. J.* **2021**, *16*, 5.
[40] S. C. Hur, A. J. Mach, D. Di Carlo, *Biomicrofluidics* **2011**, *5*, 2.